

·研究快报·

基于两种土质的暗管土工布外包料反滤效果对比试验

张迎奥¹, 王少丽², 郝瑞霞^{1*}, 荣臻³

(1. 太原理工大学水利科学与工程学院, 太原 030024; 2. 中国水利水电科学研究院水利研究所, 北京 100048; 3. 中国电建集团华东勘测设计研究院有限公司, 杭州 311122)

摘要:为了研究土质状况对暗管土工布外包料反滤效果的影响机制,该研究选取安徽蚌埠地区粉土、宁夏平罗地区砂粉土和4种热熔纺黏丝无纺布进行了室内土柱试验,对比测试了两种土壤在不同土工布防护措施下的流量、土壤和土工布渗透性变化过程,并对土工布的透水和防淤堵性能做出评价,同时从颗粒迁移的角度出发,对流量随时间变化出现先下降后上升再下降的现象(“驼峰”现象)进行了成因分析。结果表明,砂粉土土质与单位面积质量为68 g/m²的土工布、粉土土质与单位面积质量为90 g/m²的土工布之间的适配性较好,土工布能够通过颗粒筛选的方式将织物上方土壤特征粒径 d_{90} 值(小于该粒径值的土壤颗粒质量分数为90%)提升20%以上,诱导其表面高透水性土壤骨架的形成。“驼峰”现象是土壤颗粒迁移和土工布颗粒筛选二者共同作用下的结果,表征了土壤与土工布之间出现了良好的适配性。研究成果可为安徽蚌埠、宁夏平罗以及相似土质地区暗管排水土工布外包滤料的选择提供技术支持。

关键词:暗管排水; 土工布; 土质; 渗透性; 防淤堵; 颗粒迁移

doi: 10.11975/j.issn.1002-6819.202211200

中图分类号: S276.1

文献标志码: A

文章编号: 1002-6819(2023)-02-0270-07

张迎奥,王少丽,郝瑞霞,等. 基于两种土质的暗管土工布外包料反滤效果对比试验[J]. 农业工程学报, 2023, 39(2): 270-276. doi: 10.11975/j.issn.1002-6819.202211200 <http://www.tcsae.org>

ZHANG Ying'ao, WANG Shaoli, HAO Ruixia, et al. Comparative test on the anti-filtration effect of geotextile envelope material around subsurface drainage pipe using two kinds of soil[J]. Transactions of the Chinese Society of Agricultural Engineering (Transactions of the CSAE), 2023, 39(2): 270-276. (in Chinese with English abstract) doi : 10.11975/j.issn.1002-6819.202211200 <http://www.tcsae.org>

0 引言

当下,中国农业生产仍面临着涝渍盐碱等诸多问题^[1-4]。暗管排水作为一种农田排水工程措施,是指在田间地表下适当位置埋设能透水的暗管以控制地下水位、调节土壤水分和理化性状,在防止土壤退化、改造涝渍地和盐碱地等方面发挥着重要的作用^[5-7]。为防止土壤颗粒在水流冲刷作用下淤积在管内,降低暗管工程运行年限,施工中需要在管道周围加设额外防护。为解决砂石滤料取材难和造价高的问题,以丙烯等化学纤维为生产材料的土工布已逐渐成为了砂石滤料以外的最佳防护措施^[8-9]。与砂石滤料作用类似,土工布可以通过纤维织物层起到反滤作用,以减缓暗管流量衰减速度,延长暗管的使用寿命^[10-11]。但土工布材质轻薄且表面孔隙细小致密,土壤颗粒往往会堵塞或淤积在织物层表面和内部,产生淤堵^[12-13]。土工布淤堵程度与土质状况有关,稳定性较差的土壤,土工布淤堵程度将更为严重^[14]。暗管排水流量出现的先下降后上升再下降的现象,曲线形态类似驼峰(后文简称“驼峰”现象),可在

一定程度上反映出土工布良好的反滤性能对排水系统的反馈效果。不同土质状况下土工布所表现出的反滤效果将影响到“驼峰”现象是否发生,但目前有关该方面的研究还比较少;如何结合颗粒迁移来解释土壤和土工布渗透性与流量之间的响应关系,也鲜有相关报导;中国国土面积大,有农田排水需求的地区,其土质状况往往存在差异,土工布的适配性有待深入探讨。

安徽蚌埠和宁夏平罗地区分别面临着涝渍地和盐碱地改造问题,前者区域内暗管埋深处以粉土为主,后者则以砂粉土为主,土壤颗粒组分的不同导致其土质状况存在差异。因此本文以两个地区的土壤为例,选取4种热熔纺黏丝无纺布,采用室内土柱试验,对不同土工布防护措施下的流量、土壤各层和土工布渗透性变化过程进行分析,探究土质状况对土工布外包料反滤效果的影响机制,同时以颗粒迁移为切入点,分析“驼峰”现象的产生原因,并在此基础上从透水和防淤堵等方面出发,对暗管外包土工布的选取给出合理建议,以期为安徽蚌埠、宁夏平罗以及相似土质地区暗管排水土工布外包滤料的选择提供依据。

1 材料与方法

1.1 研究区概况及土样分析

安徽蚌埠位于淮北平原,区域内土质均一且渗透性较差的特点使得该地区作物极易遭受涝渍威胁^[15-16]。位于西北内陆的宁夏平罗地区,区域内土壤中粉砂颗粒含

收稿日期: 2022-11-23 修订日期: 2023-01-14

基金项目: 国家自然科学基金项目(52079145); 宁夏重点研发计划重大项目(2018BBF02022)

作者简介: 张迎奥,研究方向为农田排水与水环境保护技术。

Email: zhangyingao1027@163.com

※通信作者: 郝瑞霞,博士,教授,研究方向为水力学及河流动力学。

Email: haoruixia@tyut.edu.cn

量高，渗透性较强，地下水位在降水的补给下迅速上升，加重了土壤表层的盐碱化程度^[17]。虽然两个地区的气候条件、土质状况存在差异，但都对农田排水有着较高的需求。

试验供试土壤：①粉土（安徽蚌埠地区土壤）：取自安徽省水利科学研究院新马桥农水综合实验站试验田1.2 m埋深处；②砂粉土（宁夏平罗地区土壤）：取自宁夏回族自治区银北灌区平罗县渠口乡农耕地1.2 m埋深处，土壤质地参照1987年公布的中国土壤质地分类制进行分类^[18]。经初步筛分后，通过中国丹东百特仪器有限公司生产的型号为BT-9300HT激光粒度分析仪对供试土壤粒径组成进行测定，土壤颗粒级配曲线见图1，土壤颗粒组成及特征粒径见表1。

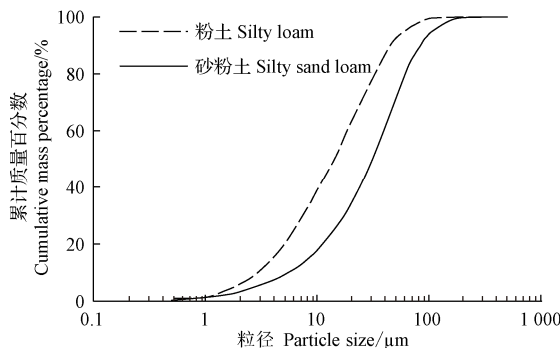


图1 土壤颗粒级配曲线

Fig.1 Soil particle gradation curve

表1 土壤颗粒组成及特征粒径

Table 1 Soil particle composition and characteristic particle size

土壤 Soil	质量分数 Mass fraction/%			d_{10}	d_{60}	d_{90}
	黏粒 Clay	粉粒 Silt	砂粒 Sand	/μm	/μm	/μm
粉土 Silty loam	6.59	84.87	8.54	2.93	18.5	46.34
砂粉土 Silty sand loam	3.36	69.39	27.25	5.51	38.3	83.72

注： d_{10} 、 d_{60} 和 d_{90} 表示小于该粒径值的土壤颗粒体积含量占比分别为10%、60%和90%。下同。

Note: d_{10} , d_{60} , and d_{90} indicate soil particle content smaller than these particle sizes of 10%, 60%, and 90%, respectively. Same below.

经计算，粉土和砂粉土中黏粒含量与粉粒含量的比值分别为0.078和0.048，土壤的不均匀系数Cu分别为6.31和6.95，土壤的粘结性和稳定性均较差，排水暗管需要包裹反滤材料^[19]。

1.2 土工布物理参数

结合相关学者的暗管土工布外包滤料研究成果^[20-21]，选取了4种规格的热熔纺黏丝无纺布进行试验，各方案编号及土工布物理参数见表2。通过室内定水头法测得粉土、砂粉土的渗透系数分别为 0.36×10^{-4} 和 1.01×10^{-4} cm/s，试验所选取的土工布渗透系数均为受保护土壤渗透系数的10倍以上，同时其 O_{90}/d_{90} （ O_{90} 为等效孔径，μm）值均大于1，满足规定要求，可开展暗管外包滤料试验^[14]。

1.3 试验装置与操作流程

试验装置如图2所示，上部为内径11 cm、高40 cm的有机玻璃圆筒，用于装填土壤，下部为半球形圆柱筒，进行排水和排砂，上、下两部分通过法兰相连，法兰中间可夹持滤网并铺设土工布。1#~2#、2#~3#和3#~4#

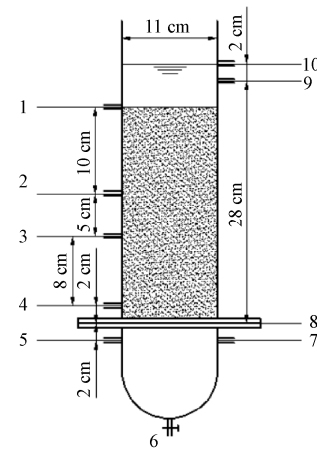
测压管分别测定上层10 cm、中层5 cm和下层8 cm土壤的渗透系数，4#~5#测压管测定土工布的渗透系数。

表2 土工布物理参数

Table 2 Geotextile physical parameters

方案 Plan	质量 Mass /(g·m ⁻²)	厚度 Thickness /mm	等效孔径 Effective aperture $O_{90}/\mu\text{m}$	渗透系数 Permeability coefficient/(cm·s ⁻¹)
A50/N50	50	0.28	360	5.6×10^{-2}
A68/N68	68	0.35	230	4.4×10^{-2}
A90/N90	90	0.38	180	3.6×10^{-2}
A120/N120	120	0.48	120	4.5×10^{-2}

注：方案中A代表粉土，N代表砂粉土，数字表示土工布单位面积质量。
Note: In plan, A represents silty loam, N represents silty sand loam, and the number indicates the quality of the geotextile unit area.



1~5.测压管 6.排砂孔 7.出流孔 8.土工布 9.进水孔 10.溢流孔
1-5.Piezometer tubes 6.Sand discharge hole 7.Outflow hole 8.Geotextiles
9.Water inlet hole 10.Overflow hole

图2 土柱渗透装置

Fig.2 Soil column infiltration device

试验按照粉土 1.3 g/cm^3 和砂粉土 1.45 g/cm^3 的天然容重逐层填装土壤，期间通过凿毛处理以使得各个土层接触密实。土壤装填完毕后，采取自下而上的注水方式向装置内部进行注水。为避免注水时水流过快扰动土壤结构以及土壤排气不及时造成的土柱断层现象，注水速度应缓慢且注水时长需控制在48 h以上。注水期间土体内会有部分气体进入到测压管内，可使用吸水球排出。待土壤充分饱和且所有测压管示数一致后，打开9#进水孔向装置内部自上而下供水，并通过10#溢流孔控制积水深度。试验期间每隔8 h记录一次流量和测压管示数，每天观测3次，取平均值作为当天测量结果，连续10 d流量无明显变化时结束试验，其中方案N50、N90和N120试验时长为35 d，其余方案试验时长65 d。

1.4 数据处理与测试指标

为避免人工装土导致的试验误差和单次试验的偶然性，将各组试验观测的流量统一修正为初始土壤渗透系数一致的情况下进行分析，土壤和土工布的渗透系数依据达西渗透定律进行计算^[22-23]。试验结束后，停止供水，打开6#排砂孔进行排水，过滤并收集沉积在下部半球圆柱筒内的土壤颗粒，排砂孔滤出的土壤颗粒加上7#出流孔排水期间滤出土壤颗粒的总和作为土壤流失量；排水完毕后，将装置平放并打开法兰，轻轻揭下土工布，刮除表面浮土后

进行烘干称量, 土工布及其截留土壤颗粒的总质量减去土工布净质量作为土工布淤堵量; 用刀片在土工布上方土壤表面(约0~3 mm范围)刮下土样薄层并烘干研磨, 其粒度分析结果可用来评判土工布的防淤堵性能。

2 结果与分析

2.1 流量变化过程

定义某一变量(流量、土壤或土工布渗透系数)残余度为某天的测量值与初始测量值的比值。图3为粉土和砂粉土在不同土工布防护作用下流量的变化过程。排水初期, 土壤颗粒会在渗透水流带动下逐渐向下进行迁移和填充孔隙, 由于土壤的不断密实和土工布的逐渐淤堵, 各方案流量均出现大幅衰减。15 d后, A50、A68、A90、A120、N50、N68、N90和N120的系统流量残余度分别为69.6%、70.4%、73.2%、67.3%、81.7%、83.7%、81.4%和79.4%。15~20 d期间, A50、A68、A90和N68的流量开始上升, 其余方案则仍然在缓慢下降。35 d后, 四组方案基本都达到了流量峰值, 峰值流量残余度分别为79.15%、76.58%、86.45%和88.08%, 其中A90和N68均维持了较长时间的流量峰值, 峰值时长分别为15 d和25 d, A50和A68在35 d达到流量峰值后便开始缓慢下降。由于N50、N90和N120未出现类似N68的流量波动且在25~35 d期间流量基本趋于稳定, 故按照试验操作流程在35 d时结束三组试验的观测。

总体上看, 出现“驼峰”现象的方案均能够在整个试验期间保持着较高的流量, 相比于砂粉土, 粉土的土质状况更容易引起“驼峰”现象的发生。

2.2 土壤和土工布渗透性变化过程

以出现“驼峰”现象的N68和A90为例, 未出现“驼峰”现象但试验时长相同的A120作为对照, 对三组方案上层10 cm、中层5 cm、下层8 cm土壤和土工布的渗透性变化过程进行分析, 如图4所示。

初始阶段, 土壤颗粒受渗流作用会产生有方向性的迁移, 土壤内部将发生孔隙填充和颗粒重新排列, 土壤密实度增加和土工布逐渐淤堵使得土壤和土工布渗透性均出现不同幅度的衰减。10~15 d期间, 三组方案上、

中层土壤渗透性先后上升, 出现“驼峰”现象的N68和A90下层土壤渗透性在15 d和20 d上升, 分别对应其流量上升时间节点; 土工布渗透性出现类似于“倒驼峰”的变化趋势, 土工布渗透系数残余度分别从46.62%、48.23%回升至59.1%、60.5%, 而未出现“驼峰”现象的A120, 其下层土壤和土工布渗透性在整个试验期间一直处于缓慢下降状态。

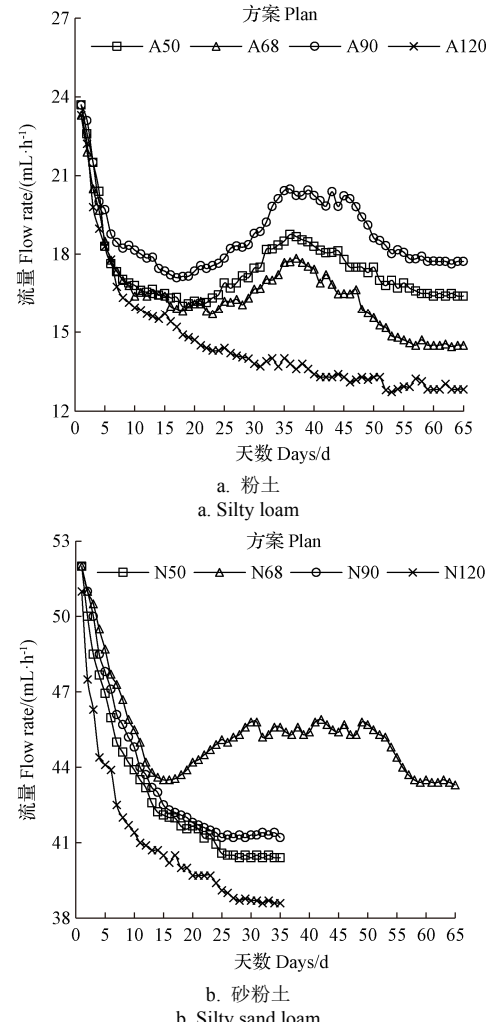
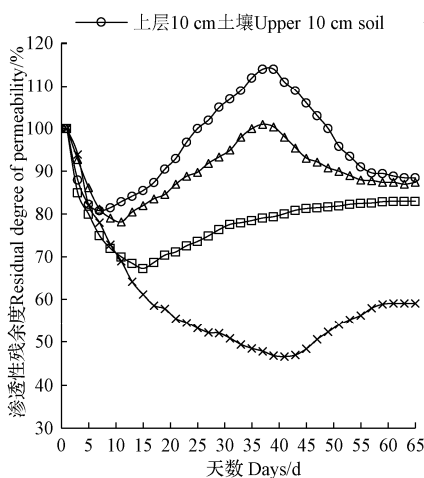
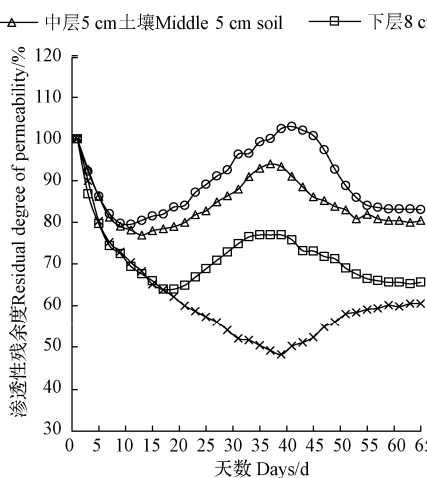


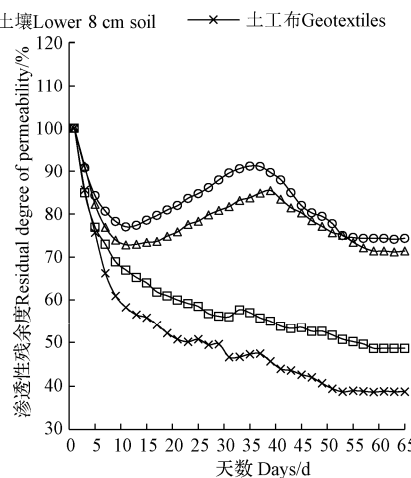
图3 粉土和砂粉土在不同土工布防护作用下的流量变化过程
Fig.3 Flow change process of silty loam and silty sand loam under the protection of geotextiles of different specifications



a. N68



b. A90



c. A120

图4 方案N68、A90和A120上层10 cm、中层5 cm、下层8 cm土壤和土工布的渗透性变化过程

Fig.4 Permeability variation of upper 10 cm, middle 5 cm and lower 8 cm soil and geotextile of plans N68, A90 and A120

表3为三组方案上10 cm、中5 cm、下8 cm土壤和土工布的渗透性变化与流量变化过程在95%置信区间的多元回归分析结果。 R^2 和方差分析F值显示三组方案回归方程关系显著,N68和A90回归方程中下层土壤和土工布的回归系数更大,说明下层土壤和土工布渗透性变化与流量变化的数量关系显著,其在流量变化过程中具备较高的决策程度,而A120中土工布渗透性则成为影响流量变化的主要决策因素。在多元回归分析

中,标准化系数常用以判别自变量在回归方程中的重要性,相比上层和中层土壤,N68和A90下层土壤和土工布的渗透性对流量变化的影响更重要,A120显示出土工布渗透性比土壤渗透性更为重要。*t*检验结果表明,引起流量变化的因素主要集中在下层土壤和土工布渗透性变化上,其*t*值大、显著性高,上层土壤渗透性显著性较低,而中层土壤渗透性中存在不显著($P>0.05$)的情况。

表3 多元回归分析结果
Table 3 Results of multiple regression analysis

方案 Plan	回归方程 Regression equations	R^2	F值 <i>F</i> value	x_1		x_2		x_3		x_4	
				标准化系数 Standard coefficients	<i>t</i> 值 <i>t</i> value						
N68	$Y=0.231x_1-0.155x_2+0.763x_3+0.553x_4+4.130$	0.97	513*	0.335	6.597*	-0.215	-2.726*	0.841	41.165*	0.633	29.033*
A90	$Y=0.215x_1+0.102x_2+0.889x_3+0.637x_4-0.866$	0.96	293*	0.297	7.668*	0.148	1.398	0.891	46.36*	0.775	26.035*
A120	$Y=-0.039x_1+0.027x_2+0.353x_3+0.718x_4+6.366$	0.99	1589*	-0.171	-4.675*	0.112	3.923*	0.584	23.44*	0.873	58.631*

注: * $P<0.05$ (65个实测值); x_1 、 x_2 、 x_3 和 x_4 分别为上层10 cm、中层5 cm、下层8 cm土壤和土工布的渗透系数残余度,%; Y 为流量残余度, %。

Note: * $P<0.05$ (65 measured values); x_1 , x_2 , x_3 , and x_4 are the residual degree of permeability coefficient of upper 10 cm, middle 5 cm and lower 8 cm soil and geotextile respectively, %; Y is drainage flow residual, %.

2.3 土工布防淤堵性能及反滤效果

表4为粉土和砂粉土在不同土工布防护下的土壤流失量和土工布淤堵量。A68和N68采用相同土工布且试验时长一致,但前者的土工布淤堵量略小于后者,而A50、A90和A120尽管试验时间长,但土工布淤堵量均小于相同土工布防护下的砂粉土方案。再者,除N50、N90和N120试验时间短造成土壤流失量相较粉土方案偏低以外,N68的土壤流失量也略低A68。结合两种土质之间的差异,粉土土壤流失量普遍高于砂粉土的原因是粉土中黏、粉粒等细颗粒占比较高,存在较多数量的土壤颗粒穿过土工布发生流失行为,而砂粉土中砂粒等粗颗粒占比明显高于粉土,土壤颗粒容易被拦截至土工布纤维织物层内部,呈现较高的土工布淤堵量,说明土质状况能够在一定程度上影响土工布的防淤堵性能。

表4 土壤流失量和土工布淤堵量

Table 4 Soil loss and geotextile clogging

方案 Plan	土工布厚度 Geotextile thickness/mm	土壤流失量 Soil loss/g	土工布淤堵量 Geotextile clogging/g
A50	0.28	1.97	0.88
A68	0.35	1.88	0.97
A90	0.38	1.56	0.53
A120	0.48	0.87	1.44
N50	0.28	1.67	1.51
N68	0.35	1.73	1.09
N90	0.38	1.04	1.68
N120	0.48	0.59	1.81

土工布上方土壤粒径分布是评价土工布对土壤反滤效果的有效指标^[24],表5为土工布上方0~3 mm范围内土壤粒度分析结果。除A120外,其余方案土工布上方土壤颗粒组成相对于原始土壤均呈现黏、粉粒含量下降,而砂粒含量上升。适配土壤的土工布作为暗管外包滤料时,其纤维织物层能够起到拦截粗颗粒放行细颗粒的作用,诱导暗管周围土壤形成以砂粒等粗颗粒搭建的具有较高渗透性的土壤透水骨架^[25]。N68和A90土工布淤堵

程度最低且 d_{90} 值明显增大,差异性分析结果显示N68和A90土工布上方黏粒、粉粒含量下降程度和砂粒含量上升程度与其他方案差异显著,说明两组方案使用的土工布分别对砂粉土和粉土两种土质表现出了良好的反滤性能。方案A120使用的土工布厚度大且致密,在渗流作用下粉土中较多数的黏、粉粒等细小土壤颗粒会逐渐迁移并累积至土工布表面,使得A120土工布上方黏、粉粒含量上升进而形成透水性极差的“滤饼”层。WEGGEL等^[26]研究发现,土工布上方一旦形成滤饼,会通过持续吸纳更小土壤颗粒的方式来逐渐增加滤饼厚度。土工布表面滤饼的形成会导致排水系统整体渗透性的下降,A120土工布上方土壤 d_{90} 值降低了1.53%,表明其表面已具备形成滤饼的条件。

表5 土工布上方0~3 mm范围内土壤粒度分析结果

Table 5 Soil particle size analysis results within 0-3 mm above the geotextile

方案 Plan	质量分数 Mass fraction/%			$d_{90}/\mu\text{m}$	d_{90} 变幅 Amplitude of $d_{90}/\%$
	黏粒 Clay	粉粒 Silt	砂粒 Sand		
A50	5.09±0.37 ^b	79.81±0.63 ^c	15.10±0.32 ^b	52.25	12.76
A68	5.19±0.27 ^b	81.33±0.55 ^b	13.48±0.45 ^c	51.33	10.77
A90	4.92±0.21 ^b	76.72±0.41 ^d	18.36±0.75 ^a	55.82	20.46
A120	6.93±0.24 ^a	85.64±0.74 ^a	7.43±0.66 ^d	45.63	-1.53
N50	3.33±0.32 ^a	69.10±0.43 ^a	27.57±1.26 ^b	84.76	1.24
N68	2.45±0.41 ^b	62.17±0.95 ^b	35.38±0.81 ^a	101.31	21.01
N90	2.71±0.31 ^{ab}	65.67±0.67 ^{ab}	31.62±0.77 ^{ab}	90.93	8.61
N120	2.53±0.22 ^b	67.20±0.71 ^a	30.27±0.69 ^b	89.13	6.46

注: 不同小写字母表示不同方案在0.05水平差异显著。

Note: Different lowercase letters indicate significant differences of different plans at the 0.05 level.

3 讨论

土壤中的细颗粒极易随水分的运移而发生迁移,且该现象多发生在松散堆积体中^[27-29]。挖沟铺管后,其回填土的压实度往往不会太大,渗流作用下土壤颗粒同样会发生剥离、运移和沉淀等迁移行为。排水初期,各层

土壤出现颗粒重新排列和孔隙填充现象以适应渗透水流, 土壤内部孔隙度降低引起渗透性下降。随着颗粒迁移过程的推进, 上层和中层土壤内部颗粒迁出量大于迁入量时, 孔隙度先后增加继而引起渗透性上升。土壤颗粒最终会迁移至下层土壤内部和土工布上方, 而适配土壤的土工布凭借错综复杂的纤维结构, 可通过放行细颗粒、拦截粗颗粒的颗粒筛选形式, 逐渐在土工布上方构建高透水性土壤骨架, 进而极大程度上改善下层土壤内部的渗流环境。试验后期部分土层渗透性再次下降, 考虑到是土壤渗流结构因颗粒迁移而到达临界状态, 难以在渗流作用下继续维持, 继而再度发生土壤颗粒重新排列和孔隙填充^[30-31]。土壤颗粒迁移和土工布通过颗粒筛选构建高透水性土壤骨架引起排水流量上升, 土壤渗流结构达到临界状态发生崩解引起排水流量下降, 在这种综合效应下, 最终排水流量呈现出了“驼峰”现象。

相对于砂粉土, 粉土土质中黏、粉粒等细颗粒含量高, 使其允许部分迁移至土工布表面的土壤颗粒发生流失, 因此粉土的土质状况更容易出现“驼峰”现象。而砂粉土中砂粒含量高使得其能够建立相对稳定的土壤渗流结构以保证在较长时间内维持流量峰值。

无论何种土质, 透水效果表现最好的往往不是等效孔径最大的土工布。粉土方案中 A50 和 A68 的流量低于 A90, 砂粉土方案中 N50 的流量低于 N68。A50 和 A68 的 O_{90}/d_{90} 值分别为 7.8 和 5.0, 过大的等效孔径导致部分应该用于搭建透水骨架结构的土壤颗粒发生流失, 因此其表现出的透水效果不如 A90。N50 土工布较大的等效孔径造成较大幅度的土壤流失量, 但随着时间的推移, 砂粉土中砂粒等粗颗粒逐渐被拦截至织物层内部, 从而形成较高的土工布淤堵量。

由于目前对土壤结构研究的限制, 难以对渗流作用下土壤颗粒的迁移进行动态追踪, 本次研究也只能结合颗粒迁移下土壤和土工布渗透性变化对“驼峰”现象进行初步分析, 期待以后借助荧光示踪等技术对该现象进行更深层次的研究。

4 结 论

1) 针对两种土质, 相同土工布表现出的透水和反滤性能存在差异。对于砂粉土土质, 50、90 和 120 g/m² 土工布出现较大幅度的淤堵情况; 对于粉土土质, 120 g/m² 土工布表面有形成滤饼的趋势。

2) 土工布的等效孔径和厚度能反映出织物拦截颗粒的能力。等效孔径和厚度均合适的土工布能够允许部分随渗流迁移下来的土壤颗粒发生流失以促进织物表层高透水性土壤骨架的形成, 但不能以流失颗粒为目的而选用较大孔隙的土工布, 否则易导致用于构建透水骨架的粗颗粒发生流失, 降低其透水能力。

3) “驼峰”现象形成原因主要与下层土壤和土工布之间颗粒动态迁移所引起的渗透性变化有关。土工布可通过颗粒筛选的方式诱导织物上方高透水性土壤骨架的形成, 从而极大地改善下层土壤的渗流环境。

4) 出现“驼峰”现象的方案均能够在整个试验期间

保持着较高的流量, 且土工布上方土壤 d_{90} 值(小于该粒径值的土壤颗粒质量分数为 90%)明显增大, 表明通过“驼峰”现象来判断土壤和土工布之间适配性是否良好是可行的。

5) 从不同土工布表现出的反滤能力上来看, 宁夏平罗地区砂粉土土质与单位面积质量为 68 g/m² 的土工布、安徽蚌埠地区粉土土质与单位面积质量为 90 g/m² 的土工布之间的适配性最好。

[参 考 文 献]

- [1] 王少丽, 许迪, 陈皓锐, 等. 农田除涝排水技术研究综述[J]. 排灌机械工程学报, 2014, 32(4): 343-349.
WANG Shaoli, XU Di, CHEN Haorui, et al. Review on research of farmland drainage technology[J]. Journal of Drainage and Irrigation Machinery Engineering, 2014, 32(4): 343-349. (in Chinese with English abstract)
- [2] 俄有浩, 马玉平. 农田涝渍灾害研究进展[J]. 自然灾害学报, 2022, 31(4): 12-30.
E Youhao, MA Yuping. Advances in research on cropland waterlogging disaster[J]. Journal of Natural Disasters, 2022, 31(4): 12-30. (in Chinese with English abstract)
- [3] 周利颖, 李瑞平, 苗庆丰, 等. 河套灌区不同掺沙量对重度盐碱土壤水盐运动的影响[J]. 农业工程学报, 2020, 36(10): 116-123.
ZHOU Liying, LI Ruiping, MIAO Qingfeng, et al. Effects of different sand ratios on infiltration and water-salt movement of heavy saline-alkali soil in Hetao irrigation area[J]. Transactions of the Chinese Society of Agricultural Engineering (Transactions of the CSAE), 2020, 36(10): 116-123. (in Chinese with English abstract)
- [4] 张美恩, 王春乙, 宋艳玲, 等. 河南省夏花生生育期旱涝灾害危险性评价[J]. 农业工程学报, 2022, 38(1): 158-168.
ZHANG Meien, WANG Chunyi, SONG Yanling, et al. Risk assessment of summer peanut drought and waterlogging disaster during growth periods in Henan Province of China[J]. Transactions of the Chinese Society of Agricultural Engineering (Transactions of the CSAE), 2022, 38(1): 158-168. (in Chinese with English abstract)
- [5] 谭攀, 王士超, 付同刚, 等. 我国暗管排水技术发展历史、现状与展望[J]. 中国生态农业学报, 2021, 29(4): 633-639.
TAN Pan, WANG Shichao, FU Tonggang, et al. Development history, present situation, and the prospect of subsurface drainage technology in China[J]. Chinese Journal of Eco-Agriculture, 2021, 29(4): 633-639. (in Chinese with English abstract)
- [6] 尹广生, 王祥, 陈冲, 等. 暗管排水技术治理盐碱地的研究进展[J]. 灌溉排水学报, 2022, 41(Supp. 2): 45-51.
YIN Guangsheng, WANG Xiang, CHEN Chong, et al. Review of subsurface drains on the control of saline-alkali land[J]. Journal of Irrigation and Drainage, 2022, 41(Supp. 2): 45-51. (in Chinese with English abstract)
- [7] 王少丽, 李益农, 陶园, 等. 太阳能光伏暗管排水系统能力提升[J]. 农业工程学报, 2022, 38(4): 99-104.
WANG Shaoli, LI Yinong, TAO Yuan, et al. Capacity improvement of solar photovoltaic subsurface pipe drainage system[J]. Transactions of the Chinese Society of

- Agricultural Engineering (Transactions of the CSAE), 2022, 38(4): 99-104. (in Chinese with English abstract)
- [8] GHANE E, DIALAMEH B, ABDALAAL Y, et al. Knitted-sock geotextile envelopes increase drain inflow in subsurface drainage systems[J]. Agricultural Water Management, 2022, 274: 107939.
- [9] 陈名媛, 黄介生, 曾文治, 等. 外包土工布暗管排盐条件下水盐运移规律[J]. 农业工程学报, 2020, 36(2): 130-139. CHEN Mingyuan, HUANG Jiesheng, ZENG Wenzhi, et al. Characteristics of water and salt transport in subsurface pipes with geotextiles under salt discharge conditions[J]. Transactions of the Chinese Society of Agricultural Engineering (Transactions of the CSAE), 2020, 36(2): 130-139. (in Chinese with English abstract)
- [10] YANNOPOULOS S I, GRISMER M E, BALI K M, et al. Evolution of the materials and methods used for subsurface drainage of agricultural lands from antiquity to the present[J]. Water, 2020, 12(6): 1767.
- [11] BAHÇECİ I, NACAR A S, TOPALHASAN L, et al. A new drainpipe-envelope concept for subsurface drainage systems in irrigated agriculture[J]. Irrigation & Drainage, 2018, 67(supp.): 40-50.
- [12] DU C, XU C, YANG Y, et al. Filtration performance of nonwoven geotextile filtering fine-grained soil under normal compressive stresses[J]. Applied Sciences, 2022, 12(24): 12638.
- [13] NIEĆ J, SPYCHAŁA M, MAZURKIEWICZ J. Septic tank effluent pretreatment using different filter materials as a prevention from clogging[J]. Environment Protection Engineering, 2016, 19(1): 15-25.
- [14] STUYT L, DIERICKX W. Design and performance of materials for subsurface drainage systems in agriculture[J]. Agricultural Water Management, 2006, 86(1/2): 50-59.
- [15] 陈金华, 刘瑞娜, 吴文革, 等. 江淮不同亚区冬小麦涝渍害气候风险时空演变[J]. 灌溉排水学报, 2022, 41(6): 121-130. CHEN Jinhua, LIU Ruina, WU Wen'ge, et al. Spatiotemporal variation of climate-induced waterlogging for winter wheat in Jianghuai Region[J]. Journal of Irrigation and Drainage, 2022, 41(6): 121-130. (in Chinese with English abstract)
- [16] 王成雨, 慕丽, 李森郁, 等. 拔节期水分冗余胁迫对淮北平原夏玉米产量形成机制的影响[J]. 农业工程学报, 2022, 38(2): 87-94. WANG Chengyu, MU Li, LI Senyu, et al. Effects of water redundancy stress at the jointing stage on the yield formation mechanism of summer maize in Huabei Plain of China[J]. Transactions of the Chinese Society of Agricultural Engineering (Transactions of the CSAE), 2022, 38(2): 87-94. (in Chinese with English abstract)
- [17] 王雁, 田生昌, 左忠. 宁夏盐碱地改良暗管排水脱盐效果研究[J]. 宁夏大学学报, 2021, 42(4): 456-462. WANG Yan, TIAN Shengchang, ZUO Zhong. Research of desalting effect of improved underground drainage pipe in saline-alkali soil of Ningxia[J]. Journal of Ningxia University, 2021, 42(4): 456-462. (in Chinese with English abstract)
- [18] 吴克宁, 赵瑞. 土壤质地分类及其在我国应用探讨[J]. 土壤学报, 2019, 56(1): 227-241.
- WU Kening, ZHAO Rui. Soil texture classification and its application in China[J]. Acta Pedologica Sinica, 2019, 56(1): 227-241. (in Chinese with English abstract)
- [19] OJAGHLOU H, SOHRABI T, RAHIMI H, et al. Laboratory study of the soil clay percent influence on the need for subsurface drainage system envelopes[C]// 9th World Congress of the International Commission of Agricultural Engineering. Quebec, Canada: American Society of Agricultural and Biological Engineers, 2010.
- [20] 胡玲玲, 杨树青, 梁志航, 等. 河套灌区下游排水暗管外包料筛选试验研究[J]. 灌溉排水学报, 2022, 41(4): 141-148. HU Lingling, YANG Shuqing, LIANG Zhihang, et al. An experimental study on wrapping materials of subsurface drain for farmland in the downstream Hetao Irrigation District[J]. Journal of Irrigation and Drainage, 2022, 41(4): 141-148. (in Chinese with English abstract)
- [21] 李杰, 王红雨, 王亚, 等. 基于回归水再利用的农田排水暗管外包滤料选型试验[J]. 节水灌溉, 2022(11): 18-25. LI Jie, WANG Hongyu, WANG Ya, et al. An Experimental investigation of envelopes filter material based on reuse of returned water from subsurface drainage tubing[J]. Water Saving Irrigation, 2022(11): 18-25. (in Chinese with English abstract)
- [22] 刘文龙, 罗纨, 贾忠华, 等. 黄河三角洲暗管排水土工布外包滤料的试验研究[J]. 农业工程学报, 2013, 29(18): 109-116. LIU Wenlong, LUO Wan, JIA Zhonghua, et al. Experimental study on geotextile envelope for subsurface drainage in Yellow River Delta[J]. Transactions of the Chinese Society of Agricultural Engineering (Transactions of the CSAE), 2013, 29(18): 109-116. (in Chinese with English abstract)
- [23] 荣臻, 王少丽, 郝瑞霞, 等. 宁夏银北灌区排水暗管土工布外包料透水与防淤堵性能[J]. 农业工程学报, 2021, 37(8): 68-75. RONG Zhen, WANG Shaoli, HAO Ruixia, et al. Permeability and anti-clogging performance of geotextile envelope material around subsurface drainage pipe in Yinbei Irrigation District in Ningxia[J]. Transactions of the Chinese Society of Agricultural Engineering (Transactions of the CSAE), 2021, 37(8): 68-75. (in Chinese with English abstract)
- [24] KALORE S A, SIVAKUMAR B G. Improved design criteria for nonwoven geotextile filters with internally stable and unstable soils[J]. Geotextiles and Geomembranes, 2022, 50(6): 1120-1134.
- [25] 荣臻. 暗管外包料透水与防淤堵性能试验研究[D]. 太原: 太原理工大学, 2021. RONG Zhen. Experimental Research on Permeability and Anti-Clogging Performance of Envelope Material Around Drainage Tube[D]. Taiyuan: Taiyuan University of Technology, 2021. (in Chinese with English abstract)
- [26] WEGGEL J R, WARD N D. A model for filter cake formation on geotextiles: Theory[J]. Geotextiles and Geomembranes, 2012, 31(4): 51-61.

- [27] LI G, WEST A J, DENSMORE A L, et al. Connectivity of earthquake-triggered landslides with the fluvial network: Implications for landslide sediment transport after the 2008 Wenchuan earthquake[J]. Journal of Geophysical Research: Earth Surface, 2016, 121(4): 703-724.
- [28] ZHANG S, ZHANG L M, CHEN H X. Relationships among three repeated large-scale debris flows at Pubugou Ravine in the Wenchuan earthquake zone[J]. Canadian Geotechnical Journal, 2014, 51(9): 951-965.
- [29] 朱秦, 苏立君, 刘振宇, 等. 颗粒迁移作用下宽级配土渗透性研究[J]. 岩土力学, 2021, 42(1): 125-134.
ZHU Qin, SU Lijun, LIU Zhenyu, et al. Study of seepage in wide-grading soils with particles migration[J]. Rock and Soil Mechanics, 2021, 42(1): 125-134. (in Chinese with English abstract)
- [30] TCHISTIAKOV A A, KOTTSOVA A K, SHVALYUK E V, et al. Physico-chemical factors of clay particle migration and formation damage[J]. Moscow University Geology Bulletin, 2022, 77(5): 552-558.
- [31] ANNAPAREDDY V S R, SUFIAN A, BORE T, et al. Spatial and temporal evolution of particle migration in gap-graded granular soils: Insights from experimental observations[J]. Journal of Geotechnical and Geoenvironmental Engineering, 2023, 149(3): 04022135.

Comparative test on the anti-filtration effect of geotextile envelope material around subsurface drainage pipe using two kinds of soil

ZHANG Ying'ao¹, WANG Shaoli², HAO Ruixia^{1*}, RONG Zhen³

(1. College of Water Resource Science and Engineering, Taiyuan University of Technology, Taiyuan 030024, China; 2. Department of Irrigation and Drainage, China Institute of Water Resources and Hydropower Research, Beijing 100048, China; 3. Powerchina Huadong Engineering Corporation Limited, Hangzhou 311122, China)

Abstract: Geotextiles are widely used as drainage pipe envelope materials in the construction of modern farmland drainage systems, due to the many product series, stable performance, and convenient transportation. Furthermore, the complex and diverse soil conditions have gradually promoted the mechanized manufacturing technology of subsurface drainage pipes in China. However, the unreasonable selection of geotextiles can lead to serious blockages of subsurface drainage pipes in many irrigation areas, and even premature loss of drainage functions. Therefore, it is urgent to select the geotextiles suitable for the local soil characteristics in the construction of farmland subsurface drainage engineering. The drainage pipe blockage can be effectively prevented while maintaining relatively stable water permeability. In this study, a systematic comparison was conducted to clarify the anti-filtration effect of geotextile envelope material around subsurface drainage pipes. An indoor hydraulic permeability test was also carried out using four kinds of hot-melt spun-bonded nonwoven geotextiles. Two kinds of soil samples were collected from Bengbu City, Anhui Province, and Pingluo County, Ningxia Hui Autonomous Region, China. The drainage flow, soil, and geotextile permeability were measured on the two kinds of soil samples under different geotextile protection measures. The permeability and anti-clogging performance of different geotextiles were then evaluated to analyze the drainage flow that increased with time (referred to as "hump") from the perspective of particle migration. The test results showed that the infiltration water flow induced the soil particles to rearrange, and then fill the pores in the early stage of drainage, particularly after the subsurface drainage pipe was laid and the soil was backfilled. Subsequently, the permeability of soil and geotextiles was reduced significantly, leading to a decrease in the drainage flow, as the soil compactness and the gradual silting of geotextiles increased with time. With the advancement of the test process, the geotextile suitable for the soil was discharged with the fine particles (such as the clay and powder particles) through particle screening, whereas, some coarse particles (such as sand particles) were intercepted with the fabric pores. As such, a well-permeable soil permeable skeleton was gradually formed around the drainage pipe, which in turn triggered the rise of drainage flow. At the same time, the test found that the equivalent pore size of geotextile failed to measure the permeability performance. Specifically, the equivalent pore size of the geotextile was too large to easily make the soil skeleton with the sand, as the construction material was damaged, causing the drainage flow. Excellent adaptability between the soil and geotextiles was observed in the silty sand loam in the Pingluo area of Ningxia and geotextiles with a mass of 68 g per unit area, while the silty loam in the Bengbu area of Anhui and geotextiles with a mass of 90 g per unit area. The characteristic particle size (d_{90}) of soil above the geotextile increased by more than 20%, compared with the original soil. In addition, the experiment also successfully verified whether the soil and geotextile fit well, according to the "hump" phenomenon. Once the "hump" phenomenon occurred, it infers that the drainage system maintained the higher permeability for a long time, indicating the better water permeability and anti-sedimentation performance of geotextile. It was different from the continuous decline of the drainage flow caused by the geotextile siltation. Consequently, the geotextiles can be expected to screen the soil characteristics in the two target areas. The findings can provide a theoretical basis and technical support to optimize the subsurface drainage pipe envelope materials in similar irrigation areas.

Keywords: subsurface drainage; geotextiles; soil properties; permeability; anti-clogging; particle migration